

**Studies on Production of Valuable Aromatics Benzene,
Toluene and Ethylbenzene Using Multiphase Catalytic
Pyrolysis of Waste Expanded Polystyrene**



**Thesis submitted in partial fulfillment
For the Award of Degree**

Doctor of Philosophy

By

Anjali Verma

**DEPARTMENT OF CHEMICAL ENGINEERING & TECHNOLOGY
INDIAN INSTITUTE OF TECHNOLOGY
(BANARAS HINDU UNIVERSITY)
VARANASI-221005**

Roll No: 17041002

2022

Copyright © Indian Institute of Technology

(Banaras Hindu University),

Varanasi - 221005, India.

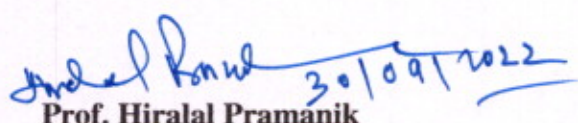
All rights reserved

2022

CERTIFICATE

It is certified that the work contained in the thesis titled “**Studies on Production of Valuable Aromatics Benzene, Toluene and Ethylbenzene Using Multiphase Catalytic Pyrolysis of Waste Expanded Polystyrene**” by “**Anjali Verma**” has been carried out under my/our supervision and that this work has not been submitted elsewhere for a degree.

It is further certified that the student has fulfilled all the requirements of Comprehensive Examination, Candidacy and SOTA for the award of Ph.D. Degree.


30/09/2022

Prof. Hiralal Pramanik

(Supervisor)

Department of Chemical
Engineering & Technology
Indian Institute of Technology
(Banaras Hindu University)

Varanasi-221005, India

प्राचार्य/Professor

रासायनिक अभियांत्रिकी एवं प्रौद्योगिकी विभाग

Deptt. of Chemical Engg. & Tech.


भारतीय प्रौद्योगिकी संस्थान

Indian Institute of Technology

काशी हिन्दू विश्वविद्यालय

Banaras Hindu University

वाराणसी/Varanasi-221005


30/09/2022

Dr. Sweta

(Co-supervisor)

Department of Chemical
Engineering & Technology
Indian Institute of Technology
(Banaras Hindu University)

Varanasi-221005, India

सहायक प्राचार्य

Assistant Professor

रासायनिक अभियांत्रिकी एवं प्रौद्योगिकी विभाग

Deptt. of Chemical Engg. & Tech.

भारतीय प्रौद्योगिकी संस्थान

Indian Institute of Technology

काशी हिन्दू विश्वविद्यालय

Banaras Hindu University

वाराणसी/Varanasi-221005

DECLARATION BY THE CANDIDATE

I, "**Anjali Verma**", certify that the work embodied in this thesis is my own bona fide work and carried out by me under the supervision of **Prof. Hiralal Pramanik** and co-supervision of **Dr. Sweta** from "July 2017 to October 2022" at the "Department of Chemical Engineering & Technology", Indian Institute of Technology (BHU), Varanasi. The matter embodied in this thesis has not been submitted for the award of any other degree/diploma. I declare that I have faithfully acknowledged and given credits to the research workers wherever their works have been cited in my work in this thesis. I further declare that I have not willfully copied any other's work, paragraphs, text, data, results, etc., reported in journals, books, magazines, reports dissertations, theses, etc., or available at websites and have not included them in this thesis and have not cited as my own work.

Date: 30/09/2022

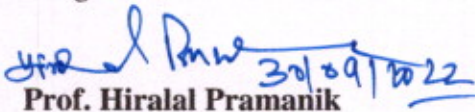
Place: Varanasi

Anjali Verma
30/09/2022

(Anjali Verma)

CERTIFICATE BY THE SUPERVISOR

It is certified that the above statement made by the student is correct to the best of my/our knowledge.

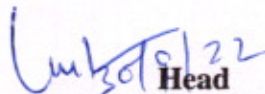

Prof. Hiralal Pramanik

(Supervisor)

Department of Chemical
Engineering & Technology
Indian Institute of Technology
(Banaras Hindu University)
Varanasi-221005, India

प्राचार्य / Professor

रासायनिक अभियांत्रिकी एवं प्रौद्योगिकी विभाग
Dept. of Chemical Engg. & Tech.
भारतीय प्रौद्योगिकी संस्थान
Indian Institute of Technology
काशी हिन्दू विश्वविद्यालय
Banaras Hindu University
वाराणसी / Varanasi-221005

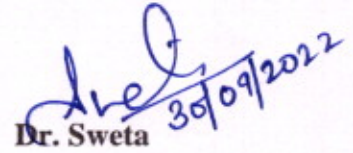

Head

(Prof. V. L. Yadav)

Department of Chemical Engineering & Technology
Indian Institute of Technology (Banaras Hindu University)
Varanasi-221005

विभागाध्यक्ष / Head

रासायनिक अभियांत्रिकी एवं प्रौद्योगिकी विभाग
Deptt. of Chemical Engg. & Tech.
भारतीय प्रौद्योगिकी संस्थान / Indian Institute of Technology
काशी हिन्दू विश्वविद्यालय / Banaras Hindu University
वाराणसी / Varanasi-221005


Dr. Sweta

(Co-supervisor)

Department of Chemical
Engineering & Technology
Indian Institute of Technology
(Banaras Hindu University)
Varanasi-221005, India

सहायक प्राचार्य
Assistant Professor

रासायनिक अभियांत्रिकी एवं प्रौद्योगिकी विभाग
Dept. of Chemical Engg. & Tech.
भारतीय प्रौद्योगिकी संस्थान
Indian Institute of Technology
काशी हिन्दू विश्वविद्यालय
Banaras Hindu University
वाराणसी / Varanasi-221005

COPYRIGHT TRANSFER CERTIFICATE

Title of the Thesis: “Studies on Production of Valuable Aromatics Benzene, Toluene and Ethylbenzene Using Multiphase Catalytic Pyrolysis of Waste Expanded Polystyrene”

”

Name of the student: Ms. Anjali Verma

Copyright Transfer

The undersigned hereby assigns to the Indian Institute of Technology (Banaras Hindu University) Varanasi all rights under copyright that may exist in and for the above thesis submitted for the award of the “**Ph.D. Degree**”.

Date: 30/09/2022

Place: Varanasi

Anjali Verma
30/09/2022
(Anjali Verma)

Note: However, the author may reproduce or authorize others to reproduce material extracted verbatim from the thesis or derivative of the thesis for author's personal use provided that the source and the Institute's copyright notice are indicated.

Dedicated to My Beloved

Parents &

Family Members

ACKNOWLEDGEMENT

I take this opportunity to express my deep sense of gratitude and indebtedness to my esteemed supervisor **Prof. Hiralal Pramanik** and Co-supervisor **Dr. Sweta** who helped enormously and always inspired me by his indispensable guidance and encouragement during the whole long research work. They always supported and strengthened me in many direct and indirect ways.

I also express my heartiest thanks to **Prof. V. L. Yadav**, Head of the Department, Department of Chemical Engineering & Technology, Indian Institute of Technology (BHU) for providing essential research facilities and encouragement during the research work.

I would especially thank **Prof. Y. C. Sharma**, Department of Chemistry and **Prof. M.K. Mondal**, Department of Chemical Engineering & Technology, Indian Institute of Technology, Banaras Hindu University. Without the help of them, my project may not be completed. I am very thankful for their valuable advice & guidance, **RPEC, DPGC members** of the Chemical Engineering & Technology Department for their useful suggestions during my research work at the institute. The instrumental facilities from CIFIC (IIT-BHU) Varanasi are gratefully acknowledged.

Also, I express my sincere thanks to all faculty members of the Department of Chemical Engineering and Technology, Indian Institute of Technology (Banaras Hindu University) for their continued help and co-operation in the completion of this research work.

I am very thankful to all technical and non-technical staff of the Department of Chemical Engineering & Technology, Institute of Technology, and Banaras Hindu University.

I also owe my sincerest thanks to my seniors and friends Mr. Pramendra Gaurh, Mr. Uday kumar Gupta, Mr. Abhay Kumar choudhary, Mr. Abhay Pratap Singh, and Mr. Neeraj kumar Yadav for their valuable help and support in the experiment, data analysis and presentation in the thesis as well as papers over the years.

The whole credit of my achievements goes to my father Mr. Vinod Kumar Verma, mother Smt. Krishna Verma, brother Ankit Verma and husband Mr. Aryan Verma who were always there for me in my difficulties. It was their unshakable faith in me that has always helped me to proceed further.

Finally, I wish to extend warm thanks to all those who could not find a separate name but have helped directly or indirectly.

Above all, I am especially thankful to the Almighty God from whom I gathered the strength and perseverance during my research work.

Date: 30/09/2022

Place: Varanasi

Anjali Verma
30/09/2022
(Anjali Verma)

TABLE OF CONTENTS

List of Figures	xiv-xviii
List of Tables	xix-xxii
Nomenclature	xxiii-xxiv
Preface	xxv-xxx i
CHAPTER 1 INTRODUCTION	1-11
CHAPTER 2 LITERATURE REVIEW AND RESEARCH OBJECTIVES	12-45
2.1 Literature review	12
2.1.1 Raw materials	12
2.1.1.1 Feedstock for the pyrolysis process	12
2.1.1.1.1 Feed characterization	14
2.1.1.2 Catalysts for pyrolysis	15
2.1.1.2.1 Catalyst characterization	21
2.1.2 Types of reactor/design	29
2.1.3 Types of pyrolysis process	31
2.1.3.1 Thermal pyrolysis	31
2.1.3.2 Catalytic pyrolysis	33
2.1.4 Mechanism for the formation of BTE via thermal and catalytic pyrolysis	34
2.1.5 Factors affecting the BTE production from PS	37
2.1.5.1 Production of BTE via thermal pyrolysis of PS	37
2.1.5.2 Production of BTE via catalytic pyrolysis of PS	40
2.1.6 Pyrolysis product characterization	42
2.2 Objectives	44

CHAPTER 3: EXPERIMENTAL	46-61
3.1 Materials	46
3.2 Experimental setup	48
3.3 Method	51
3.3.1 Feed preparation	51
3.3.2 Feed characterization	52
3.3.2.1 Proximate analysis	52
3.3.2.2 Thermogravimetry analysis (TGA)	53
3.3.3 Catalyst synthesis from natural red clay	53
3.3.4 Catalyst characterization	54
3.3.4.1 Scanning electron microscope-energy dispersive X-ray spectroscopy (SEM-EDX)	55
3.3.4.2 X-ray diffraction (XRD)	55
3.3.4.3 Brunauer-Emmet-Teller (BET) surface area	55
3.3.4.4 Fourier transformed infra-red spectroscopy (FTIR)	56
3.3.5 Pyrolysis process for the production of BTE	56
3.3.6 Catalyst regeneration	57
3.4 Pyrolysis oil analysis	58
3.4.1 Gas chromatography (GC) analysis	58
3.4.1.1 Estimation of BTE and styrene in pyrolysis oil	58
3.4.2 FTIR of pyrolysis oil	59
3.4.3 Physicochemical properties	59
3.4.3.1 Gross calorific value (GCV)	59

3.4.3.2 Carbon residue	60
3.4.3.3 Flash and fire point	60
CHAPTER 4: OPTIMIZATION OF PROCESS PARAMETERS USING RSM	62-69
4.1 Introduction	62
4.2 Optimization using RSM-BBD	67
CHAPTER 5: RESULTS AND DISCUSSION	70-189
5.1 Feed characterization	71
5.1.1 Proximate analysis of WEPS	71
5.1.2 Thermo-chemical behaviour of WEPS	71
5.2 Thermal pyrolysis of WEPS: Part I	73
5.2.1 Effect of process parameters on product yield	73
5.2.1.1 Effect of temperature and holding time	73
5.2.1.2 Effect of heating rate	75
5.2.1.3 Effect of temperature	76
5.2.2 Analysis of thermal pyrolysis oil	77
5.2.2.1 Estimation of aromatic content/BTE and styrene in pyrolysis oil	77
5.2.2.2 FTIR analysis of thermal pyrolysis oil	80
5.2.2.3 Physicochemical properties of thermal pyrolysis oil	82
5.3 Catalytic pyrolysis of waste expanded polystyrene (WEPS): Part II	84
5.3.1 Catalytic pyrolysis using ZSM-5 ammonium powder as catalyst	84
5.3.1.1 Effect of process parameters on product yield	84
5.3.1.1.1 Effect of feed to catalyst ratio	84

5.3.1.1.2 Effect of temperature and holding time	86
5.3.1.1.3 Effect of heating rate	88
5.3.1.1.4 Effect of temperature	90
5.3.1.2 Analysis of pyrolysis oil obtained using ZSM-5 ammonium powder catalyst	93
5.3.1.2.1 Estimation of aromatic content/BTE and styrene in pyrolysis oil	93
5.3.1.2.2 FTIR analysis of pyrolysis oil	99
5.3.1.2.3 Physicochemical properties of pyrolysis oil	101
5.3.2 Catalytic pyrolysis using Nickel on silica-alumina as catalyst	102
5.3.2.1 Effect of process parameters on product yield	102
5.3.2.1.1 Effect of feed to catalyst ratio	102
5.3.2.1.2 Effect of temperature and holding time on liquid and solid yield	104
5.3.2.1.3 Effect of heating rate	106
5.3.2.1.4 Effect of temperature	108
5.3.2.2 Analysis of pyrolysis oil obtained using Nickel on silica-alumina catalyst	110
5.3.2.2.1 Estimation of aromatic content/BTE and styrene in pyrolysis oil	110
5.3.2.2.2 FTIR analysis of pyrolysis oil	115
5.3.2.2.3 Physicochemical properties of pyrolysis oil	117
5.3.3 Catalytic pyrolysis using synthesized catalyst from natural red clay	118
5.3.3.1 Catalyst characterization	118
5.3.3.1.1 SEM-EDX analysis	118
5.3.3.1.2 BET surface area analysis	121
5.3.3.1.3 XRD analysis	124
5.3.3.1.4 FTIR analysis of red clay catalysts	127

5.3.3.2 Selection of best catalyst among all synthesized red clay catalysts	128
5.3.3.3 Effect of process parameters on product yield	130
5.3.3.3.1 Effect of feed to catalyst ratio	130
5.3.3.3.2 Effect of temperature and holding time	132
5.3.3.3.3 Effect of heating rate	134
5.3.3.3.4 Effect of temperature	135
5.3.3.4 Analysis of pyrolysis oil obtained using RC-800 catalyst	138
5.3.3.4.1 Estimation of aromatic content/BTE and styrene in pyrolysis oil	138
5.3.3.4.2 FTIR of pyrolysis oil	143
5.3.3.4.3 Physicochemical properties of pyrolysis oil	145
5. 4 Performance comparison of three catalysts for the BTE production	147
5.5 Process parameters through RSM	149
5.5.1 RSM coupled with BBD for maximization of liquid yield	149
5.5.1.1 Optimization of process variables	160
5.5.1.1.1 Optimization of process variables using ZSM-5 ammonium powder	160
5.5.1.1.2 Optimization of process variables using Nickel on silica-alumina catalyst	164
5.5.1.1.3 Optimization of process variables using best red clay catalyst RC-800	168
5.5.2 Analysis of pyrolysis oil	172
5.5.2.1 Qualitative analysis of pyrolysis oil obtained using three different catalysts	172
5.5.2.2 Physicochemical properties of pyrolysis oil obtained using three different catalysts	177
5.6 Regeneration and reusability study of catalyst	178

5.6.1 Reusability assessment of best catalyst Nickel on silica-alumina catalyst	179
5.6.1.1 Characterization of regenerated catalyst Nickel on silica-alumina	179
5.6.1.1.1 SEM analysis	179
5.6.1.1.2 BET surface area analysis	181
5.6.1.2 Product yield of AB-type pyrolysis	181
5.6.1.3 Analysis of pyrolysis oil	183
5.6.1.3.1 Quantification of aromatic content/BTE and styrene in pyrolysis oil	183
5.6.1.3.2 Physicochemical properties of pyrolysis oil	184
6. CONCLUSIONS	189-198
REFERENCES	199-218
Appendix A1	219
Appendix A2	220
Appendix A3	221
Appendix A4	223
Appendix A5	224
Appendix A6	226
Appendix A7	227
Appendix A8	229

LIST OF FIGURES

Figure 1.1	Growth in global plastic production	2
Figure 1.2	Applications of pyrolysis process	6
Figure 2.1	Schematic drawing of the structure of ZSM-5	16
Figure 2.2	Structure of a 1:1 clay mineral layer (a) and of a 2:1 clay mineral layer (b) (the interlayer cations are depicted on the schematic drawing of the layered structure on the left) T = tetrahedral sheet, O = octahedral sheet, d_L = basal spacing of the crystal	19
Figure 2.3	Physisorption isotherm classification	23
Figure 2.4	XRD pattern of Nb_2O_5 and NiO/Nb_2O_5 catalyst	24
Figure 2.5	py-FTIR of Nb_2O_5 and NiO/Nb_2O_5 catalyst	25
Figure 2.6	SEM images of plain and metal oxide impregnated catalyst (a) WBKD and (b) $ZnO/WBKD$	26
Figure 2.7	FTIR of different kaoline clay K325 (325 mesh of kaolin), K800 (800 mesh of kaolin), K1250 (1250 mesh of kaolin), K325-M (325 mesh of modified kaolin), K800-M (800 mesh of modified kaolin), K1250-M (1250 mesh of modified kaolin)	27
Figure 2.8	XRD of different kaoline clay K325 (325 mesh of kaolin), K800 (800 mesh of kaolin), K1250 (1250 mesh of kaolin), K325-M (325 mesh of modified kaolin), K800-M (800 mesh of modified kaolin), K1250-M (1250 mesh of modified kaolin)	28
Figure 2.9	Proposed reaction pathway for thermal cracking of polystyrene to form BTE	35
Figure 2.10	Mechanism of formation of major product during catalytic pyrolysis of EPS	36
Figure 3.1	Pictorial view of natural red clay (a) lump of red clay (b) grounded natural red clay	48
Figure 3.2	Schematic of the experimental setup for the pyrolysis of WEPS	49
Figure 3.4	Reactor arrangements (a) thermal (b) A-type/liquid phase (c) B-type/vapour phase (d) AB-type/multiphase catalytic pyrolysis	50
Figure 3.5	Detailed diagram of (a) secondary reactor (b) perforated base of secondary reactor	51
Figure 3.6	Photographic view of (a) collected waste expanded polystyrene, (b) WEPS after processing via heat treatment	52

Figure 3.7	Flow diagram for synthesis of catalyst from natural red clay	54
Figure 3.8	Calibration characteristics for benzene, toluene and ethylbenzene (BTE)	59
Figure 5.1	TGA/DTG curve of waste expanded polystyrene (WEPS)	72
Figure 5.2a	Effect of temperature on liquid and solid yield for thermal pyrolysis at 15 °C/min heating rate and zero holding time	74
Figure 5.2b	Effect of holding time on liquid and solid yield for thermal pyrolysis at a heating rate of 15 °C/min and at a temperature of 650 °C	74
Figure 5.3	Effect of heating rate on product yield obtained from thermal pyrolysis of WEPS at a temperature of 550 °C	75
Figure 5.4	Effect of temperature on product yield obtained from thermal pyrolysis of WEPS at a heating rate of 15 °C/min	77
Figure 5.5	Comparison of gas chromatographs of thermal pyrolysis oil obtained at optimum conditions with commercial fuel gasoline and kerosene	79
Figure 5.6	FTIR spectra of pyrolysis oil obtained from thermal pyrolysis of WEPS at optimum conditions	80
Figure 5.7	Effect of feed to catalyst ratio on product yield for liquid phase catalytic process/A-type at 600 °C and 15 °C/min using ZSM-5 ammonium powder catalyst	85
Figure 5.8a	Effect of temperature on liquid and solid yield for liquid phase catalytic/A-type pyrolysis at 15 °C/min heating rate and zero hold time using ZSM-5 ammonium powder catalyst	87
Figure 5.8b	Effect of holding time on liquid and solid yield for liquid phase catalytic/A-type pyrolysis at 15 °C/min and 600 °C using ZSM-5 ammonium powder catalyst	88
Figure 5.9	Effect of heating rate on product yield obtained from catalytic pyrolysis i.e., A-type, B-type and AB-type at a temperature of 550 °C using ZSM-5 ammonium powder catalyst	89
Figure 5.10	Effect of temperature on product yield obtained from catalytic pyrolysis i.e., A-type, B-type and AB-type at a heating rate of 15 °C/min using ZSM-5 ammonium powder catalyst	91
Figure 5.11a	Gas chromatographs of catalytic pyrolysis oil A-type, B-type, and AB-type obtained at optimum conditions using ZSM-5 ammonium powder catalyst	96

Figure 5.11b	Comparison of gas chromatographs of AB-type catalytic pyrolysis oil obtained using ZSM-5 ammonium powder at optimized conditions with commercial gasoline and kerosene	98
Figure 5.12	FTIR spectra of catalytic pyrolysis oil obtained at optimum conditions using ZSM-5 ammonium powder catalyst (a) A-type/liquid phase, (b) B-type/Vapour phase and (c) AB-type/multiphase	99
Figure 5.13	Effect of feed to catalyst ratio on product yield of liquid phase/A-type catalytic pyrolysis at 600 °C and heating rate of 15 °C/min using Nickel on silica-alumina catalyst	103
Figure 5.14a	Effect of temperature on liquid and solid yield for liquid phase catalytic/A-type pyrolysis at 15 °C/min heating rate and zero hold time using Nickel on silica-alumina catalyst	105
Figure 5.14b	Effect of holding time on liquid and solid yield for liquid phase catalytic/A-type pyrolysis at 15 °C/min and 600 °C using Nickel on silica-alumina catalyst	105
Figure 5.15	Effect of heating rate on product yield of catalytic pyrolysis i.e., A-type, B-type and AB-type at pyrolysis temperature of 550 °C using Nickel on silica-alumina catalyst	107
Figure 5.16	Effect of temperature on product yield for catalytic pyrolysis i.e., A-type, B-type and AB-type at a heating rate of 15 °C/min using Nickel on silica-alumina catalyst	108
Figure 5.17a	Gas chromatographs of catalytic pyrolysis oil A-type, B-type and AB-type obtained at optimum conditions using Nickel on silica-alumina catalyst	113
Figure 5.17b	Comparison of gas chromatographs of AB-type pyrolysis oil obtained at optimum conditions using Nickel on silica-alumina catalyst with commercial fuel gasoline and kerosene	114
Figure 5.18	FTIR spectrum of catalytic pyrolysis oil obtained at optimum conditions using Nickel on silica-alumina catalyst (a) A-type/liquid phase (b) B-type/vapour phase (c) AB-type/multiphase	115
Figure 5.19	SEM analysis of red clay catalysts (a) raw red clay, (b) red clay calcined at 600 °C, (c) red clay calcined at 700 °C, (d) red clay calcined at 800 °C, (e) red clay calcined at 900 °C	119
Figure 5.20	EDX analysis of red clay catalysts (a) raw red clay, (b) red clay calcined at 600 °C, (c) red clay calcined at 700 °C, (d) red clay calcined at 800 °C, (e) red clay calcined at 900 °C	121

Figure 5.21	N ₂ adsorption/desorption isotherm (a) raw red clay, (b) red clay calcined at 600 °C, (c) red clay calcined at 700 °C, (d) red clay calcined at 800 °C, (e) red clay calcined at 900 °C	122
Figure 5.22	XRD characteristics of red clay catalysts (a) raw red clay, (b) red clay calcined at 600 °C, (c) red clay calcined at 700 °C, (d) red clay calcined at 800 °C, (e) red clay calcined at 900 °C	125
Figure 5.23	FTIR analysis of raw red clay (RC) catalyst and calcined red clay catalysts RC-600, RC-700, RC-800 and RC-900 into two different frequency regions (a) 3660-3640 cm ⁻¹ (b) 1600-450 cm ⁻¹	128
Figure 5.24	Effect of feed to catalyst ratio on product yield for A-type/liquid phase catalytic process using best red clay catalyst RC-800 at a pyrolysis temperature of 600 °C and heating rate of 15 °C/min	131
Figure 5.25a	Effect of temperature on liquid and solid yield for liquid phase catalytic/A-type pyrolysis at 15 °C/min heating rate and zero hold time using red clay catalyst RC-800	132
Figure 5.25b	Effect of holding time on liquid and solid yield for liquid phase catalytic/A-type pyrolysis at 15 °C/min and 600 °C using best red clay catalyst RC-800	133
Figure 5.26	Effect of heating rate on product yield obtained from catalytic pyrolysis i.e., A-type, B-type and AB-type at a pyrolysis temperature of 550 °C using best red clay catalyst RC-800	134
Figure 5.27	Effect of temperature on product yield obtained from catalytic pyrolysis i.e., A-type, B-type and AB-type at a heating rate of 15 °C/min using best red clay catalyst RC-800	136
Figure 5.28a	Gas chromatographs of catalytic pyrolysis oil A-type, B-type and AB-type obtained at optimum conditions using RC-800 catalyst	140
Figure 5.28b	Comparison of gas chromatographs of AB-type pyrolysis oil obtained at optimum conditions using best red clay catalyst RC-800 with commercial gasoline and kerosene	142
Figure 5.29	FTIR spectrum of catalytic pyrolysis oil obtained at optimum conditions using best red clay catalyst RC-800 (a) A-type/liquid phase (b) B-type/vapour phase (c) AB-type/multiphase	144
Figure 5.30	Actual vs predicted values of the model for liquid yield using ZSM-5 ammonium powder catalyst	155
Figure 5.31	Actual vs predicted values of the model for liquid yield using Nickel on silica-alumina catalyst	157

Figure 5.32	Actual vs predicted values of the model for liquid yield using best red clay catalyst RC-800	159
Figure 5.33	Three dimensional surface response for liquid yield showing effects of (A) temperature and heating rate (B) temperature and feed to catalyst ratio (C) heating rate and feed to catalyst ratio using ZSM-5 ammonium powder catalyst	162
Figure 5.34	Three dimensional surface response for liquid yield showing effects of (A) temperature and heating rate (B) temperature and feed to catalyst ratio (C) heating rate and feed to catalyst ratio using Nickel on silica-alumina catalyst	166
Figure 5.35	Three dimensional surface response for liquid yield showing effects of (A) temperature and heating rate (B) temperature and feed to catalyst ratio (C) heating rate and feed to catalyst ratio using best red clay catalyst RC-800	170
Figure 5.36a	Comparison of gas chromatographs of multiphase catalytic pyrolysis oil obtained at optimized conditions using ZSM-5 ammonium powder catalyst with commercial gasoline and kerosene	173
Figure 5.36b	Comparison of gas chromatographs of multiphase catalytic pyrolysis oil obtained at optimized conditions using Nickel on silica-alumina catalyst with commercial gasoline and kerosene	174
Figure 5.36c	Comparison of gas chromatographs of multiphase catalytic pyrolysis oil obtained at optimized conditions using best red clay catalyst RC-800 with commercial gasoline and kerosene	175
Figure 5.37 (a-e)	SEM image of Nickel on silica-alumina (a) fresh catalyst; (b) & (c) spent catalyst after fifth run of multiphase/AB-type i.e., liquid phase (b) and vapour phase (c); regenerated catalyst of multiphase/AB-type i.e., liquid phase (d) and vapour phase (e)	180
Figure 5.38	Comparison of product yield obtained from multiphase catalytic pyrolysis of WEPS using fresh, used/spent and regenerated Nickel on silica-alumina catalyst at a temperature of 550 °C, heating rate of 15 °C/min using feed to catalyst ratio of 20:1	182

LIST OF TABLES

Table 2.1	Composition of natural red clay	21
Table 2.2	Liquid yield, BTE and styrene content obtained from the thermal pyrolysis of PS	38
Table 2.3	Liquid yield, BTE and styrene content obtained from the catalytic pyrolysis of PS	41
Table 3.1	Specifications of ZSM-5 ammonium powder catalyst	47
Table 3.2	Specifications of Nickel on silica-alumina catalyst	47
Table 4.1	Range of independent process variables	68
Table 5.1	Proximate analysis of WEPS	71
Table 5.2	TGA data of waste expanded polystyrene	72
Table 5.3	Product yield and BTE content obtained from thermal pyrolysis of WEPS in the temperature range of 400-700 °C at 15 °C/min heating rate	78
Table 5.4	Peak assignments for functional groups present in the thermal pyrolysis oil obtained at optimum conditions	81
Table 5.5	Physicochemical properties of thermal pyrolysis oil with standard fuel gasoline and kerosene	83
Table 5.6	Product yield of A-type/liquid phase catalytic pyrolysis at 600 °C and 15 °C/min using varying feed to catalyst ratio using ZSM-5 ammonium powder catalyst	86
Table 5.7	Product yield obtained from catalytic pyrolysis of WEPS using various reactor arrangements at optimum temperature and heating rate of 15°C/min using ZSM-5 ammonium powder catalyst	92
Table 5.8	Product yield and BTE content obtained from catalytic pyrolysis of WEPS in the temperature range of 400-700 °C at 15 °C/min heating rate using ZSM-5 ammonium powder catalyst	94
Table 5.9	Functional groups present in the pyrolysis oil obtained at optimum conditions using ZSM-5 ammonium powder catalyst	100

Table 5.10	Physicochemical properties of catalytic pyrolysis oil obtained at optimum conditions using ZSM-5 ammonium powder catalyst with standard commercial fuel gasoline and kerosene	102
Table 5.11	Effect of feed to catalyst ratio on product yield of liquid phase/A-type catalytic pyrolysis at 600 °C and heating rate of 15 °C/min using Nickel on silica-alumina catalyst	104
Table 5.12	Product yield of catalytic pyrolysis at optimum temperature using Nickel on silica-alumina catalyst	109
Table 5.13	Aromatics BTE content of catalytic pyrolysis in the range of temperature 400 °C -700 °C and at the heating rate of 15 °C/min using Nickel on silica-alumina catalyst	111
Table 5.14	Functional groups present in the catalytic pyrolysis oil obtained at optimum conditions using Nickel on silica-alumina catalyst	116
Table 5.15	Physicochemical properties of catalytic pyrolysis oil obtained at optimum conditions using Nickel on silica-alumina catalyst	118
Table 5.16	Surface concentration of various elements obtained by EDX analysis of raw and calcined red clay catalyst	120
Table 5.17	BET surface area and silica-alumina content of synthesized red clay catalysts	123
Table 5.18	Comparison between liquid yield and BTE content obtained all types of red clay catalyst i.e., RC, RC-600, RC-700, RC-800, RC-900	129
Table 5.19	Product yield of A-type/liquid phase catalytic pyrolysis at 600 °C and 15 °C /min using varying feed to catalyst ratio using best red clay catalyst RC-800	131
Table 5.20	Product yield of WPES pyrolysis using various types of reactor arrangements at optimum temperature and heating rate of 15 °C/min using best red clay catalyst RC-800	137
Table 5.21	Product yield and BTE content obtained from catalytic pyrolysis of WEPS in the temperature range of 400 °C to 700 °C at 15 °C/min heating rate using best red clay catalyst RC-800	139
Table 5.22	Functional groups present in the pyrolysis oil obtained by catalytic pyrolysis of WEPS at optimum conditions using best red clay catalyst RC-800	145

Table 5.23	Physicochemical properties of catalytic pyrolysis oil obtained at optimum conditions using best red clay catalyst RC-800	146
Table 5.24	Comparison between liquid yield and BTE content obtained from different catalysts at optimum condition	148
Table 5.25	Box-Behnken (BBD) design matrix for three independent variables with predicted and experimental value using ZSM-5 ammonium powder as catalyst	150
Table 5.26	Box-Behnken (BBD) design matrix for three independent variables with predicted and experimental value using Nickel on silica-alumina as catalyst	151
Table 5.27	Box-Behnken (BBD) design matrix for three independent variables with predicted and experimental value using natural red clay as catalyst RC-800	152
Table 5.28	ANOVA analysis for response (liquid yield) for ZSM-5 ammonium powder as catalyst	153
Table 5.29	ANOVA analysis for response (liquid yield) for Nickel on silica-alumina as catalyst	156
Table 5.30	ANOVA analysis for response (liquid yield) for natural red clay as catalyst	158
Table 5.31	Predicted and experimental value of liquid yield at optimized condition using ZSM-5 ammonium powder as catalyst	163
Table 5.32	Predicted and experimental value of liquid yield at random conditions using ZSM-5 ammonium powder catalyst	164
Table 5.33	Predicted and experimental value of liquid yield at optimized condition using Nickel on silica-alumina catalyst	167
Table 5.34	Predicted and experimental value of liquid yield at random conditions using Nickel on silica-alumina catalyst	168
Table 5.35	Predicted and experimental value of liquid yield at optimized condition using best red clay catalyst RC-800	171
Table 5.36	Predicted and experimental value of liquid yield at random conditions using red clay catalyst RC-800	172
Table 5.37	Benzene, toluene and ethylbenzene (BTE) content in the pyrolysis oil obtained at optimized conditions from multiphase catalytic pyrolysis	177

using ZSM-5 ammonium powder, Nickel on silica-alumina, Red clay catalyst RC-800

Table 5.38	Physicochemical properties of multiphase catalytic pyrolysis oil obtained at optimum conditions using ZSM-5 ammonium powder, nickel on silica-alumina catalyst and best red clay catalyst RC-800 compared with commercial fuel gasoline and kerosene	178
Table 5.39	BET surface area of fresh, used and regenerated Nickel on silica-alumina catalyst for multiphase catalytic pyrolysis	181
Table 5.40	Product yield obtained from multiphase catalytic pyrolysis for different experimental runs using fresh, used/spent and regenerated Nickel on silica-alumina catalyst	183
Table 5.41	Aromatics BTE and styrene content of multiphase catalytic pyrolysis oil obtained using fresh, spent/used and regenerated Nickel on silica-alumina catalyst	183
Table 5.42	Physicochemical properties of pyrolysis oil obtained from multiphase catalytic pyrolysis using fresh, used and regenerated Nickel on silica-alumina catalyst	185
Table 5.43	Comparison of the present study with other pyrolysis works based on the pyrolysis of polystyrene (PS) available in the open literature	187

NOMENCLATURE

Abbreviation	Meaning
ANOVA	Analysis of variance
BBD	Box-Behnken Design
BET	Brunauer Emmett Teller
3D	Three-dimensional
DF	Degree of freedom
EDX	Energy dispersive X-ray spectroscopy
EPS	Expanded polystyrene
FTIR	Fourier transform infrared spectroscopy
GCV	Gross calorific value
HDPE	High density polyethylene
LDPE	Low density polyethylene
MPW	Municipal plastic waste
MSW	Municipal solid waste
PE	Polyethylene
PP	Polypropylene
PS	Polystyrene
RSM	Response surface methodology
SEM	Scanning Electron Microscopy
TGA	Thermogravimetry analysis

WEPS Waste expanded polystyrene

XRD X-Ray Diffraction

Greek Symbols

Meaning

δ_o Linear parameter

δ_{ii} Quadratic parameter

δ_{ij} Interaction parameter

PREFACE

The production of plastics is rapidly increasing due to its low manufacturing cost, various applications, development and modernization of society. The drastic increase in the plastic production naturally has led to large amount of plastic waste generation that is deteriorating the environment because of proper disposal plastic waste. A few options that have been considered for plastic waste management were recycling and energy recovery technique. However, several obstacles of recycling techniques such as the need of sorting process that is labour intensive and also polluting environment. Thus, the recycle process is not sustainable. In view of this, the plastic waste conversion into energy and valuable chemicals via pyrolysis process was considered in the present study to develop an economical and sustainable process through extensive research.

Recently, pyrolysis of waste expanded polystyrene (WEPS) gained much attention because of its high energy content, chemical value and low recycling rate. The polystyrene is a non-biodegradable aromatic plastic which can convert in to valuable aromatics such as benzene, toluene and ethylbenzene (BTE) via pyrolysis followed by *in-situ* hydrogenation at a moderate temperature. Thus, in the present research work, catalytic pyrolysis of waste expanded polystyrene (WEPS) followed by *in-situ* hydrogenation was conducted in three different reactor arrangements i.e., liquid phase/A-type, vapour phase/B-type and multiphase/AB-type for the production of valuable aromatics benzene, toluene and ethylbenzene (BTE) and reduction of unwanted styrene in the pyrolysis oil. The thermal pyrolysis process was also performed for comparison in terms of product yield and composition.

The raw material waste expanded polystyrene (WEPS)/thermocol was collected from the waste yard of Indian Institute of Technology (BHU), Varanasi. First of all, the large sheets of

thermocool were manually cut into small pieces of size 80 mm x 80 mm using a cutter. Thereafter, the volume was reduced by placing the cut pieces of WEPS in an oven at a temperature of 85 °C for 1 hr which resulting in brittle mass of average size 40 mm x 40 mm. Three different types of catalysts i.e., ZSM-5 ammonium powder, Nickel on silica-alumina and synthesized catalyst from natural red clay were used for the catalytic pyrolysis of WEPS for each type of reactor arrangement. First two catalysts were commercial and last one was synthesized catalyst from natural red clay. The catalyst Zeolite ZSM-5 ammonium powder of surface area 400 m²/g with SiO₂ to Al₂O₃ mole ratio of 200-400:1 was procured from Alfa Aesar, USA. The commercial catalyst ammonium ZSM-5 (SiO₂:Al₂O₃ =200-400:1) powder was used in the present study due to its excellent catalytic activity towards the formation of better liquid yield containing aromatics hydrocarbons. The ammonium type ZSM-5 also provides Bronsted acid sites NH₄⁺ which helps in selective cracking. The Nickel on silica-alumina powder with 66 ± 5 % Ni was also procured from Alfa Aesar, USA. The nickel on silica-alumina catalyst improves the hydrogen production during the pyrolysis process which, may use in *in-situ* hydrogenation reaction for the production of ethylbenzene. Furthermore, the Nickel on silica-alumina catalyst shows higher selectivity towards the gasoline range hydrocarbon molecules. The natural red clay was selected as the catalyst because of high silica (41.10 wt.%) and alumina content (31.48 wt.%) as these are responsible for the catalytic properties of red clay. The natural red clay was collected from Chandauli district of Uttar Pradesh near Devdari and Rajdari waterfall which is situated 60 km away from IIT (BHU) campus, Varanasi. Five different catalysts were synthesized from the eco-friendly and non-toxic red clay i.e., red clay in natural form (RC), red clay calcined at 600 °C (RC-600), red clay calcined at 700 °C (RC-700), red clay calcined at 800 °C (RC-800), red clay calcined at 900

°C (RC-900). The raw and calcined red clay catalysts were characterized by various characterization techniques such as scanning electron microscope/energy dispersive X-ray spectroscopy (SEM-EDX), X-ray diffraction (XRD), Brunauer-Emmet-Teller (BET) surface area, Fourier transformed infra-red spectroscopy (FTIR).

The treated waste expanded polystyrene (WEPS) of 50 g fed to the primary reactor made of mild steel of 99.3 mm inner diameter and 155 mm height. The thermal and catalytic pyrolysis of WEPS were performed at different temperatures in the range between 400 °C to 700 °C, under inert atmosphere of nitrogen (200 mL/min). The catalytic pyrolysis was performed using all three selected catalysts i.e., ZSM-5 ammonium powder, Nickel on silica-alumina and synthesized catalyst from natural red clay for each type of reactor arrangement. The catalytic pyrolysis was performed at different feed to catalyst ratio of 10:1, 20:1, 30:1 and 40:1.

Scanning electron microscopy (SEM) confirms that the calcination temperature greatly influenced the surface morphology and surface area of the red clay catalysts. The surface morphology of calcined red clay catalyst RC-800 shows nano cluster form of particles with very high porosity. The highest surface area of 29.25 m²/g and highest silica content of 56.82 wt.% were found for the RC-800 catalyst. Furthermore, the XRD analysis ensured the presence of illite-micas, α - quartz, κ - kappa alumina, δ - delta alumina, and θ - theta alumina in the RC-800 catalyst only. The presence of strong Bronsted acid sites in RC-800 catalyst was confirmed by the Fourier transform Infrared spectroscopy (FTIR) analysis. Thus, the optimum calcination temperature for red clay was found to be 800 °C, as RC-800 catalyst showed excellent catalytic activity for *in-situ* hydrogenation to obtained target molecules benzene, toluene and ethylbenzene (BTE).

The compositional analysis of pyrolysis oil was evaluated by gas chromatograph (NUCON 5765) using flame ionization detector (GC-FID). The bomb calorimeter (IP 12/63 T) was used to determine the gross calorific value (GCV) of pyrolysis oil. The carbon residue of pyrolysis oil was obtained using Rams bottom carbon residue apparatus (IP 14/65). The flash and fire point of pyrolysis oil were obtained using Cleveland open cup apparatus (ASTM D 92).

The valuable aromatics benzene, toluene, and ethylbenzene (BTE) were significantly increased and styrene got reduced by many folds when AB-type/multiphase catalytic pyrolysis was performed for each type of catalyst i.e., ZSM-5 ammonium powder, Nickel on silica-alumina and best red clay catalyst RC-800. However, the highest amount of BTE content was found in the case of Nickel on silica-alumina catalyst.

Thermal pyrolysis produced maximum liquid yield of 94.37 wt.% at a temperature of 650 °C and at a heating rate of 15 °C/min. On the other side, the catalytic pyrolysis using ZSM-5 ammonium powder produced maximum liquid yield of 88.05 wt.%, 78.85 wt.%, and 75.11 wt.% for the A-type, B-type, and AB-type catalytic pyrolysis at the temperature of 600 °C, 550 °C and 550 °C, respectively using the same heating rate of 15 °C/min. The liquid oil of thermal pyrolysis contains very low amount of valuable aromatic hydrocarbons BTE of 11.38 wt.% and the highest amount of styrene (84.74 wt.%). The BTE content of pyrolysis oil obtained using ZSM-5 ammonium powder increased progressively in the order of 18.98 wt.% (A-type) < 24.27 wt.% (B-type) < 28.12 wt.% (AB-type). The styrene content significantly decreased to a very low value of 46.30 wt.% for AB-type/multiphase pyrolysis at a reaction temperature of 550 °C, heating rate of 15 °C/min, feed to catalyst ratio of 20:1 using ZSM-5 ammonium powder catalyst.

The liquid phase/A-type, vapour phase/B-type and multiphase/AB-type catalytic pyrolysis using Nickel on silica-alumina catalyst produced a highest liquid yield of 88.54 wt.%, 83.21 wt.%, and 81.15 wt.% at the same heating rate of 15 °C/min and at a reaction temperature of 600 °C, 550 °C, and 550 °C, respectively. Among, the all types of reactor arrangements, AB-type/multiphase pyrolysis produced pyrolysis oil with highest amount of BTE content of 28.56 wt.% using Nickel on silica-alumina catalyst. Furthermore, the pyrolysis oil obtained from A-type, B-type and AB-type catalytic pyrolysis contains low styrene content of 69.94 wt.%, 65.67 wt.% and 55.55 wt.%, respectively as compared to thermal pyrolysis (84.74 wt.%).

On the other side, the highest liquid yield of 88.82 wt.% was obtained for the A-type pyrolysis at the optimum temperature of 600 °C and heating rate of 15 °C/min using red clay catalyst RC-800. The B-type and AB-type pyrolysis produced maximum liquid yield of 80.81 wt.% and 79.47 wt.% respectively, at the optimum temperature of 550 °C and at heating rate of 15 °C/min using the same red clay catalyst RC-800. However, the multiphase/AB-type pyrolysis produced highest BTE content of 27.62 wt.% and lowest styrene content (60.75 wt.%) at a temperature of 550 °C using RC-800 catalyst among all types of pyrolysis. The maximum BTE content of 23.51 wt.% and 18.58 wt.% were obtained for vapour phase/B-type and liquid phase/A-type catalytic pyrolysis at their respective optimum conditions. The styrene content got reduced significantly from 68.83 wt.% to 60.75 wt.% when the reactor arrangement was changed from A-type to AB-type.

The effective process parameters such as feed to catalyst ratio, heating rate and temperature were also optimized by ESM for the best reactor arrangement AB-type using each type of catalyst i.e., ZSM-5 ammonium powder, Nickel on silica-alumina and synthesized catalyst from natural red clay via RSM-BBD technique. The optimum value of temperature (A_1),

heating rate (B_1) and feed to catalyst ratio (C_1) suggested by model were 566.62 °C, 15.41 °C, and 20.80:1, respectively for AB-type pyrolysis using ZSM-5 ammonium powder catalyst. The predicted (Y_1) and experimental value of liquid yield were 74.73 wt.% and 74.04 wt.%, respectively at the optimized condition for the same ZSM-5 ammonium powder catalyst. However, the predicted and experimental values of maximum liquid yield (Y_2) were of 81.10 wt.% and 80.85 wt.%, respectively were obtained for the multiphase/AB-type pyrolysis at the optimum temperature (A_2) of 536.04 °C, heating rate (B_2) of 15.02 °C/min and feed to catalyst ratio (C_2) of 20.54:1 using Nickel on silica-alumina catalyst. The predicted maximum liquid yield (Y_3) of 79.49 wt.% was obtained for the optimum temperature (A_3) of 536.51 °C, heating rate (B_3) of 15.15 °C/min and feed to catalyst ratio (C_3) of 20.33:1 using best red clay catalyst RC-800. Whereas, the experimental value of response (liquid yield) was found to be 78.88 wt.% at the same optimized conditions (A_3 , B_3 , and C_3) using RC-800 catalyst.

In addition, the reusability assessment was performed using best Nickel on silica-alumina catalyst only for the best reactor arrangement multiphase/AB-type. The experiments were performed at the reaction temperature of 550 °C, heating rate of 15 °C/min and feed to catalyst ratio of 20:1. The fresh Nickel on silica-alumina catalyst produced the liquid yield of 81.15 wt.% and gaseous yield of 17.14 wt.% for AB-type catalytic pyrolysis in Run-1. Whereas, the liquid yield decreased to 87.15 wt.% at the fifth run using used/spent Nickel on silica-alumina catalyst. The surface area of fresh catalyst decreased from 96.60 m²/g to 6.35 m²/g and 7.00 m²/g for liquid phase (primary reactor) and vapour phase catalyst (secondary reactor), respectively. However, the surface area increased to 82.70 m²/g for liquid phase catalyst and 86.20 m²/g for vapour phase catalyst after the regeneration process. The BTE content of 28.56 wt.% was found for the pyrolysis oil obtained from fresh Nickel on silica-alumina catalyst at

a temperature of 550 °C, heating rate of 15 °C/min and feed to catalyst ratio of 20:1. Whereas, the BTE content was reduced to 14.27 wt.% at the fifth run (5th) of experiment. The regenerated Nickel on silica-alumina catalyst produced BTE content of 28.44 wt.% in the pyrolysis oil which is similar to the BTE content obtained using fresh catalyst.

The pyrolysis oil obtained from AB-type/multiphase reactor arrangements using Nickel on silica-alumina catalyst highest BTE content and fuel range hydrocarbon and thus, the gross calorific value of the pyrolysis oil for this catalyst was found to be highest (12750 Cal/g). The other physicochemical properties were also satisfactory for the use in IC engine, diesel generator set or cooking stoves.